KTH ROYAL INSTITUTE
OF TECHNOLOGY

Degree project in Electrical Engineering

Second cycle, 30 credits

Reconfigurable Intelligent Surfaces: Optimal Positioning and Coverage Improvement

NOÈ BERNADAS I BUSQUETS

Stockholm, Sweden 2023

Authors

Noè Bernadas i Busquets <noebib@kth.se>
Information and Communication Technology
KTH Royal Institute of Technology

Place for Project

Stockholm, Sweden
Division of Communication Systems, KTH Kista

Examiner

Emil Björnson, Professor
Division of Communication Systems
KTH Royal Institute of Technology

Supervisor

Anders Enqvist, Doctoral Student
Division of Communication Systems
KTH Royal Institute of Technology

Abstract

With the emergence of future mobile generations beyond 5G, novel technologies are studied to satisfy the envisioned requirements of future services such as Ultra-Reliable Low Latency Communications (URLLC) or Virtual Reality. Among these technologies, Reconfigurable Intelligent Surfaces (RIS) arise as one of the most promising due to their capabilities to improve the channel while only modestly increasing the network energy consumption. However, multiple challenges have to be addressed before they can be deployed. In this thesis, we study strategies for positioning the RIS to achieve maximum SNR coverage in an outdoor propagation environment. Our model takes into account the effects of shadow fading and line-of-sight (LoS). A comparison between centralized and distributed deployments is also considered. Additionally, the required size of RIS to match the coverage of a small cell is assessed. The results show that the best positions to deploy a RIS lie close to the mobile terminals, in the vicinity of the boundary between covered and out-of-coverage areas. It is concluded that a centralized deployment is better than a distributed one, and a feasible size of the RIS which matches the small cell coverage is obtained.

Keywords

6G, Reconfigurable Intelligent Surfaces, Wireless Communications, Coverage.

Abstract

Med framväxten av framtida mobilgenerationer bortom 5G, studeras nya teknologier för att tillgodose de förväntade kraven för framtida tjänster som Ultra-Reliable Low Latency Communications (URLLC) eller Virtual Reality. Bland dessa teknologier uppstår Reconfigurable Intelligent Surfaces (RIS) som en av de mest lovande på grund av deras förmåga att förbättra kanalen samtidigt som de bara ökar nätverkets energiförbrukning måttligt. Men flera utmaningar måste lösas innan de kan distribueras. I denna avhandling studerar vi strategier för att positionera RIS för att uppnå maximal SNR-täckning i en utomhusförökningsmiljö. Vår modell tar hänsyn till effekterna av skuggfading och siktlinje (LoS). En jämförelse mellan centraliserade och distribuerade distributioner övervägs också. Dessutom bedöms den nödvändiga storleken på RIS för att matcha täckningen av en liten cell. Resultaten visar att de bästa positionerna för att distribuera en RIS ligger nära de mobila terminalerna, i närheten av gränsen mellan täckta och utomtäckta områden. Man drar slutsatsen att en centraliserad distribution är bättre än en distribuerad, och en genomförbar storlek på RIS som matchar den lilla celltäckningen erhålls.

Nyckelord

6G, omkonfigurerbara intelligenta ytor, trådlös kommunikation, täckning.

Acronyms

RIS Reconfigurable Intelligent Surfaces

URLLC Ultra-Reliable Low Latency Communications

SNR Signal-to-Noise ratio

UE User Equipment

SDMA Space-Division Multiple Access

HetNet Heterogenous Networks

GBSM Geometry-Based Stochastic Models

QuaDRiGa Quadriga Channel Model

MRC Maximum-Ratio Combining

Contents

Chapter 1

Introduction

1.1 Background

With the advent of the future mobile generations beyond 5G, the data rate, latency and coverage requirements of future services are expected to increase significantly. Examples of it are Ultra-Reliable Low Latency Communications (URLLC), which will require very low latencies, or Virtual Reality, which will require very high data rates. To cope with this increase in demand, several novel technologies are being studied, e.g. Cell-Free Massive MIMO or moving to the THz band [1].

Among these technologies, one of the most promising is the so-called Reconfigurable Intelligent Surfaces (RIS), also known as metasurfaces. A RIS is a thin surface composed of an array of small antennas, usually called scattering elements, where each of these receives and re-radiates without amplification (i.e., passively) but with a reconfigurable time delay. In narrow-band communications, this time delay corresponds to a phase shift, which allows beamforming techniques to receive and transmit steering the array's radiation pattern. The reconfiguration of phase-shit is carried out by a low-consumption microcontroller following different signalling procedures with a base station.

RIS stems from the idea of improving the propagation environment of a wireless link, creating a so-called smart radio channel. However, the idea of improving the channel besides the transmitter and receiver is not new, since it is what wireless repeaters (also known as relays) do: given a zone with low coverage, a relay improves the signal reception amplifying the transmitted signal, which entails an additional power consumption. In this context, RIS arise as an interesting alternative, since amplification can be achieved only by using passive beamforming techniques [2].

Nonetheless, RIS is still a young technology with many open critical research questions to solve about their performance, from the real-time control of the RIS and the related pilot overhead problems [3] to the search of a convincing use case for it [2]. The objective of this thesis is to shed light on the improvement of SNR coverage due to RIS, studying the optimal deployment of it to achieve the best results in terms of covered area. Besides, numerical comparisons between RIS and small cells will be carried out. Small cells are base stations with reduced size, transmit power and computational capabilities compared to traditional base stations (also known as macro cells), and therefore have less range and fewer registered users.

1.2 Problem

In this thesis, the problem of optimal RIS deployment is considered. Specifically, simulations of a given out-doors urban propagation environment will be carried out considering there is a fixed base station and RIS. The objective will be to find the best position for RIS to maximize the coverage area, i.e. the area on which the Signal-to-Noise ratio (SNR) is higher than a specific SNR threshold. Additionally, numerical comparisons will be performed to check the capabilities of RIS to replace small cells. In summary, we want to answer the following questions:

1. Which is the best positioning and orientation of RIS in a propagation environment?
2. Is it better to deploy only a RIS with M elements or several with a total number of M elements?
3. How many elements does RIS need to match the coverage capabilities of a small cell?

1.3 Purpose

The main purpose of this thesis is to gain knowledge about a hypothetical future deployment of RIS in mobile communications. RIS is still a quite novel research topic and it is valuable to shed light on matters that might become relevant in the future deployment of RIS in a real use case, like the one presented in this report.

1.4 Goal

The goal of this thesis is to find the best deployment strategies of RIS for several scenarios and draw generic rules about the placement of RIS in future RIS-Aided networks. A simulation environment in Matlab is used to numerically find the best positioning of the RIS.

An expected deliverable of the project is a mathematical model of communication between the base station, the RIS and the User Equipment (UE), taking into account the fading modelling of the scenario and the directivity of RIS elements.

1.5 Benefits, Ethics and Sustainability

This project degree is scientifically relevant since it provides insights into the deployment of RIS, which is an under-researched topic that might be of interest to telecommunications service providers, equipment manufacturers and the academic research community.

Regarding ethics and sustainability, the passive nature of RIS means that they consume very small amounts of energy and future networks could be able to save energy if deploying RIS is seen as a feasible alternative to small cells in some scenarios, thus improving the efficiency and sustainability of cellular networks [4].

1.6 Methodology

This thesis is carried out at the Division of Communication Systems of KTH Royal Institute of Technology. RIS is a novel technology and the aim of this thesis is to provide some insights about a hypothetical future deployment of RIS in a cell network. In order to answer the questions of section 1.2, a MATLAB simulation environment is developed, which will follow a defined propagation model that captures the essentials of reality without becoming computationally unfeasible. The numerical results of the simulations are then used to draw conclusions on the deployment of RIS.

1.7 Delimitations

On the one hand, remark that no physical implementation will be carried out due to a lack of time and budget. On the other hand, it is not expected to simulate all the propagation physics of electromagnetic waves but a simple approximation to draw generic conclusions.

1.8 Outline

In Chapter 2, the theoretical background of RIS is discussed, from hardware considerations to signal processing, outlining the main research carried out so far regarding the research question of this thesis. In Chapter 3, all the details regarding the methodology of the research are explained, e.g. channel modelling and the scenarios to be tested, and some implementation details are introduced. In Chapter 4, the resultant plots of the research are provided. Finally, in Chapter 5, conclusions are drawn and future research lines are considered.

Chapter 2

Theoretical Background

2.1 Beamforming and Directivity

In essence, a RIS is an array of antennas. Through the usage of beamforming techniques, the RIS is able to receive and transmit a signal with a configurable radiation pattern. Next, the basic principles of array beamforming are explained.

One of the most important features of a radiation element is to which direction the power is emitted. This is summarized in the so-called directivity function $D(\theta, \phi)$, which shows how the power is distributed in polar coordinates. In this thesis, it is supposed that all the points of interest are in the far-field of the antenna, and near-field considerations are neglected.

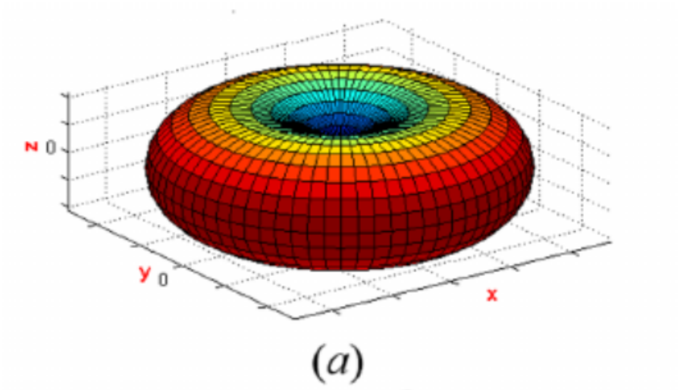

Figure 2.1: Directivity of an elemental dipole. [5]

Depending on the shape of the antenna, we obtain different directivities. The more concentrated $D(\theta, \phi)$ is around a specific direction, the more directive is the antenna. For instance, Fig. 2.2 is more directive than Fig. 2.1.

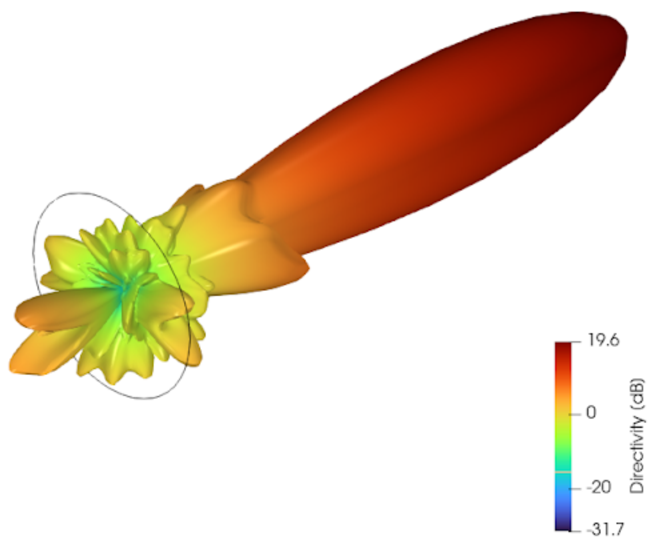

Figure 2.2: Directivity of a parabolic antenna. [6]

Once an antenna is built, the directivity cannot be changed, and if you wanted to steer the radiation pattern you would have to rely on mechanical movements, e.g. marine radars. However, in many applications, it is desired to modify the radiation pattern without depending on mechanical movements that would make real deployments more expensive and complex. In the field of mobile communications, with the advent of Space-Division Multiple Access (SDMA), the idea of having a configurable directivity gained importance [7]. In this context, the phased arrays of antennas arise as a feasible solution thanks to beamforming techniques. In essence, beamforming is based on steering the directivity using multiple antennas that transmit the same signal but with different phase shifts, leading to constructive interference in a certain direction [8].

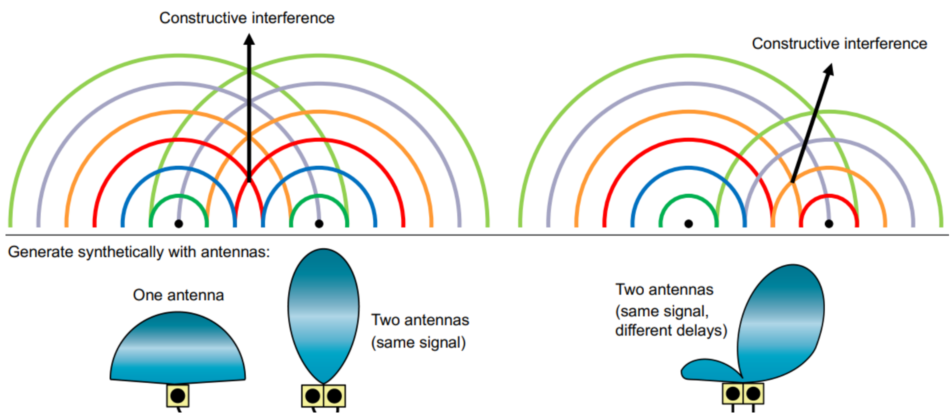

Figure 2.3: Graphical explanation of beamforming. The coloured circles are points with the same phase. [9]

With this technique, it could be possible to transmit (and, due to Lorentz reciprocity theorem, to receive) to any direction, given the proper phase shift configuration. Besides, the signal would be amplified in certain directions, since several waves would interfere constructively, but in other directions, the signal would be attenuated due to destructive interference. On the other hand, the resulting radiation pattern would also depend on the directivity of a single antenna element of the array and it can be proved that:

$$D(\theta, \phi) = D_{\text{element}}(\theta, \phi) \cdot D_{\text{array}}(\theta, \phi). \tag{2.1}$$

If the antenna elements are isotropic then $D(\theta, \phi) = D_{\text{array}}(\theta, \phi)$. The proof of 2.1 can be found in [10].

2.2 Square Law

The maximum achievable directivity in terms of power is the constructive sum of the M waves, where M is the number of elements of the array, therefore $D_{\text{max}} = M^2$. Considering uncorrelated noise between RIS elements and Maximum-Ratio Combining (MRC), an SNR improvement of M is obtained [8]. RIS use beamforming twice, for receiving the impinging signal from a base station and transmitting it to a desired UE. Therefore, RIS entails an SNR improvement of M^2, i.e. the SNR scales with the square of the RIS elements. This fact is usually referred to as the square law [2].

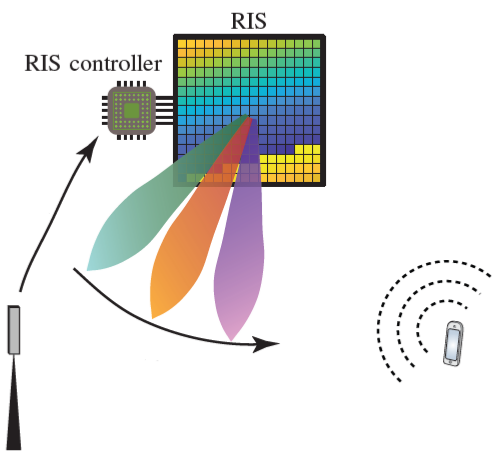

Figure 2.4: Example of RIS deployment. [9]

On the other hand, the recent advances in the electronic design of RIS have shown the economical feasibility and energy consumption efficiency that would entail the deployment of RIS with respect to previous technologies such as wireless repeaters [11] [12].

2.3 Related Work

RIS arise as one of the most promising technologies to improve the spectral efficiency of cellular networks. In the last few years, research has been carried out in order to study and address the main challenges regarding the implementation of RIS, from channel estimation [1] to the search for worthy use cases [13]. This thesis is focused on the latter. Specifically, the optimum positioning of RIS and its equivalence in terms of coverage to a small cell are studied. Small cells are a technology already implemented in LTE, in the context of Heterogenous Networks (HetNet), envisioned to improve the spectrum efficiency of a cellular network. It consists of using cells with a reduced size, transmitted power and computational capability compared to traditional macro cells, and therefore with less range and fewer registered users. However, a small cell is still an active element, with non-negligible energy consumption. With the advent of RIS, the possibility of reducing the density of small cells deployed while reducing overall energy consumption arises.

Many articles can be found on the analysis and modelling of RIS. Next, we enumerate some of the most relevant for this project. In [14], the basic principles of RIS both from physics and communications perspectives are described and it surveys research contributions that apply machine learning. In [15], it overviews RIS applications from RIS-Aided Multicell Networks to RIS-Aided cognitive radio networks. In [16], an exhaustive overview of RIS is carried out, from path loss modelling to a comparison of the performance of RIS in function of their location. In [17], an analysis of the state of the art is provided and numerical simulations are carried out to show the performance enhancement with the use of RIS in typical wireless networks. In [1], a mathematical development of the most relevant signal processing formulas in the context of wireless communications is provided. In [13], a stochastic geometry simulation scenario is analyzed to draw conclusions on the performance of RIS in the presence of randomly located blockages. In [18], a RIS-Aided Cell Free scenario is considered, and is one of the few papers, to the best of the author's knowledge, to draw clear conclusions on the capabilities of RIS to replace small cells. In this thesis, we do not consider a Cell Free scenario, but a traditional cellular network.

On the other hand, regarding the optimal positioning of RIS, the research is not abundant, and, to the best of the author's knowledge, the main references are [19], [20] and [21]. In [19] and [20], a remarkable analysis of RIS optimal placement can be found for mmWaves in indoor and outdoor scenarios, and it concludes that RIS should be closer to receivers than transmitters. However, the analysis is done in ideal free space scenarios, without taking into account the shadow fading due to the possible multiple obstacles in the propagation environment. So, in this thesis, an analysis of the optimal positioning of RIS will be performed supposing a realistic scenario with multiple obstacles and their respective shadow fading. In [21], a remarkable theoretical information theory study about distributed deployment strategies of RIS is performed, and it was concluded that centralized deployment is better than distributed. In this thesis, the conclusions of [21] will be checked by comparing the coverage of different RIS configurations: centralized and distributed, taking into account the total size of the deployed RIS.

Chapter 3

Engineering-related content, Methodologies and Methods

When it comes to the simulation of wireless networks, there is a wide variety of simulators available, each with a different level of complexity and similarity to a real deployment scenario. Regarding RIS simulation, several options have been considered so far. On the one hand, there are ray-tracing simulations which are based on the idea that, providing a digital map of the environment, a set of propagation laws are applied to obtain the resultant coverage of a deployment. This method is computationally demanding, especially for large outdoor scenarios, but it can provide the most realistic results if a real deployment is expected.

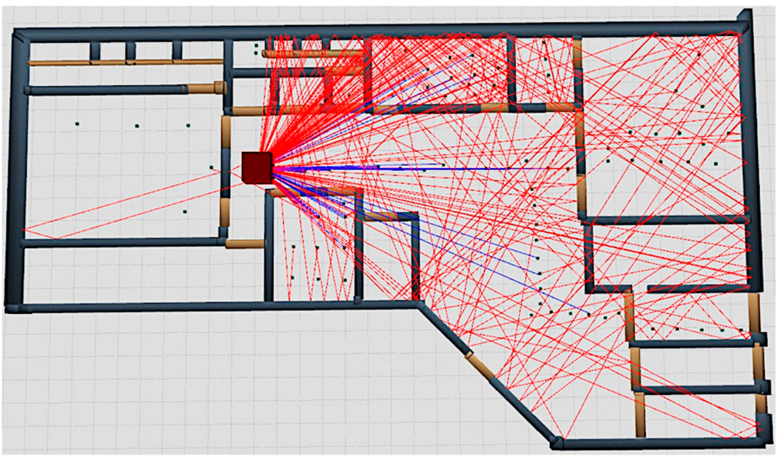

Figure 3.1: Example of ray-tracing indoor simulation. [22]

On the other hand, there are non-geometry-consistent methods which are mainly based on modelling the channel only as a probabilistic distribution (e.g. Rician).

This simplification becomes really useful when studying, for instance, RIS channel estimation algorithms [23] or qualitative comparisons between RIS and relays [24].

There is still another option, the Geometry-Based Stochastic Models (GBSM), which offers a trade-off between the fully-deterministic ray-tracing and stochastic methods. GBSM does not need the exact map of the environment, like ray-tracing, as the position of scatterer clusters is generated randomly according to calibrated distributions. After the cluster generation, ray-tracing can be applied. Additionally, Large and Small Scale fading parameters can be introduced. A paradigmatic example of GBSM is Quadriga Channel Model (QuaDRiGa), a MATLAB open-source simulator by Fraunhofer Heinrich-Hertz-Institute [25].

In this thesis, it was decided to implement a simplistic ray-tracing model in MATLAB. The non-geometry-consistent methods do not take into account the geometry of the environment, which is a really important point when assessing the SNR coverage. On the other hand, GBSM might become useful in the study of RIS [26], but it is unclear how coverage could be studied, and due to the lack of time, finally ray-tracing was chosen. Next, the details of the implemented simulator are explained.

3.1 Scenario: Shadow Fading and LOS/NLOS

First of all, the dimensions of the environment are 300x300 meters. A BS is placed at the point (300,300). To define the obstacles, a correlated urban shadow-fading map with respect to the BS is generated with QuaDRiGa. With this map, we are able to model the presence of obstacles for the BS. In order to model the shadow-fading for the RIS, we define circular obstacles placed in a coherent way with the SF map of the BS, see Fig. 3.2. The idea of this is to determine which points are in LoS with the RIS and change the path loss model accordingly. One might wonder why not another SF map for the RIS is generated. The main reason is that SF maps of BS and RIS should be correlated with each other, and this is not a trivial question: Quadriga is not able to generate so. Therefore, this alternative solution is considered. In Fig. 3.3, we can see an example of the different zones we obtain given a RIS placed in (150,50). Depending on the zone, a different channel model is applied. The same applies if a small cell is deployed instead of RIS.

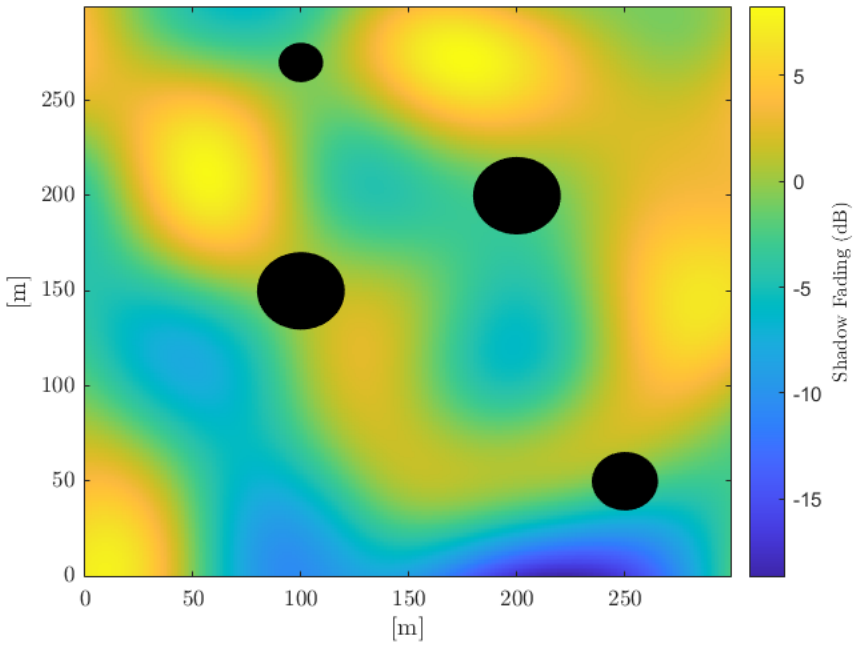

Figure 3.2: Example of shadow fading map with respect to BS in (300,300). In black, the added obstacles.

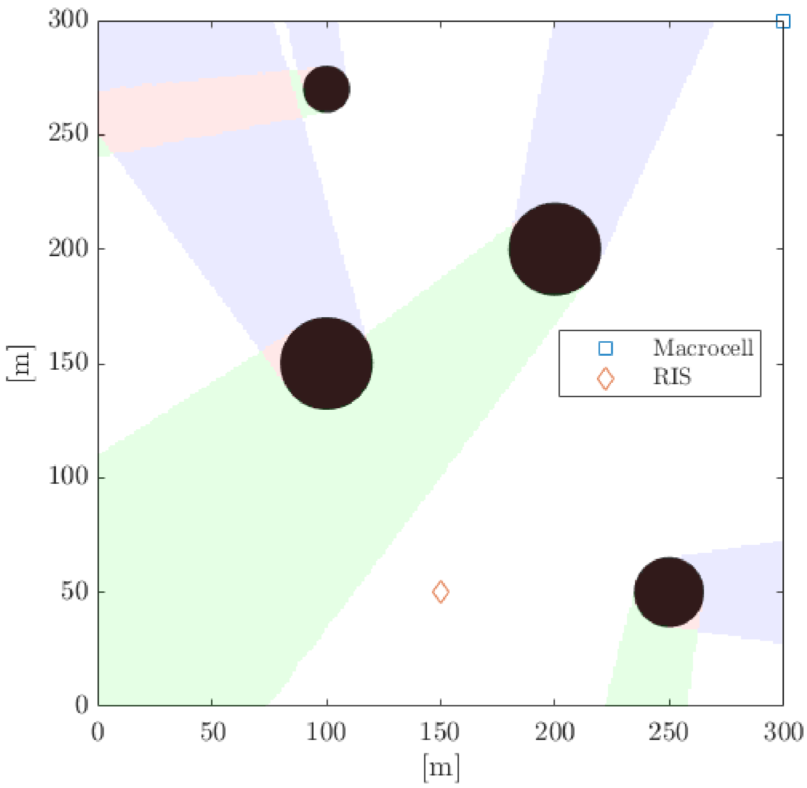

Figure 3.3: Map of zones. Green: LOS RIS - NLOS BS. Blue: NLOS RIS - LOS BS. Red: NLOS RIS - NLOS BS.

3.2 Channel model

The channel model is deterministic, i.e. is only dependent on the relative distance between the transmitter and receiver. It is supposed that proper signal processing techniques are applied to obtain a flat-fading narrowband channel without fast fading, in order to have a simple simulation environment.

3.2.1 Base station channel model

An NLOS path loss is implemented (3GPP 38.901 UMa NLOS). The base station transmits with a central frequency of 3.5 GHz and 100 W of power. The thermal noise power is computed from the formula $P_n = k_B{\cdot}T{\cdot}B$, where k_B is Boltzmann's constant, T is the temperature, supposed to be 290 K, and B is the bandwidth, supposed to be 100 MHz. An isotropic antenna is considered. The path loss equation is

$$P_{\text{NLOS}}(dB) = -32.4 - 20{\cdot}\log_{10}(f_c/10^9) - 30{\cdot}\log_{10}(d). \tag{3.1}$$

3.2.2 RIS channel model

Two path losses are implemented (38.901 UMa LOS and NLOS). Note that with RIS we have two paths defined: from BS to RIS and from RIS to UE. Depending on the relative distance to UE, BS and obstacles, a LOS or NLOS path loss is applied for each path. The path loss equations are

$$P_{\text{LOS}}(dB) = -28 - 20{\cdot}\log_{10}(f_c/10^9) - 22{\cdot}\log_{10}(d) \tag{3.2}$$

$$P_{\text{NLOS}}(dB) = -32.4 - 20{\cdot}\log_{10}(f_c/10^9) - 30{\cdot}\log_{10}(d). \tag{3.3}$$

Next, in this thesis electrically small RIS are considered, that is, RIS is small compared to transmission distances. Therefore, according to [14], the path losses of BS to RIS and RIS to UE are multiplied (distance product model). Due to the square law mentioned in Chapter 2, the number of elements M squared of the RIS scales the resultant power. Therefore, the UE would receive the following power from the RIS:

$$P_{\text{RX}} = \frac{K}{r_{\text{BS}}^{k_1}{\cdot}r_{\text{UE}}^{k_2}}{\cdot}M^2{\cdot}D_{\text{BS}}{\cdot}D_{\text{RIS element}}{\cdot}D_{\text{UE}} \tag{3.4}$$

where K, k_1 and k_2 are determined by the previous path loss equations and $D_{BS}, D_{\text{RIS element}}$ and D_{UE} are the directivity values of the BS, RIS element and UE. BS and UE are supposed to be isotropic, so $D_{BS} = D_{UE} = 1$. r_{BS} and r_{UE} are the distance from BS to RIS and from RIS to UE.

Next, we suppose that the system manages to sum coherently the signal directly from the BS and from the RIS to the UE. Given the following channel gain expression of a UE receiving from the BS and a RIS:

$$g = p + \sum_{m=1}^{M} e^{-j \cdot c_n} b_{1,m} \cdot b_{2,m} \tag{3.5}$$

where $p \in \mathbb{C}$ is the channel gain of the direct path BS-UE and $b_{1,m}, b_{2,m} \in \mathbb{C}$ is the channel gain for each element of RIS from BS and to UE respectively. Then, it is proven at [3] that g is maximized if:

$$c_n = arg(p) - arg(b_{1,m} \cdot b_{2,m}). \tag{3.6}$$

Therefore:

$$g = |p| + |b_{1,m} \cdot b_{2,m}|. \tag{3.7}$$

Eq. 3.6 and 3.7 entail two assumptions. First, it is supposed the BS has perfect knowledge of the state of the channel, which is an optimistic situation since the real control and channel estimation of RIS is still an open research question. This is though not a critical assumption since the main point of this thesis is the study of the optimal deployment. Second, the quantization effects of phase shift c_n are neglected. In the case of having multiple RIS, we suppose that all sum coherently. In other works, links between RIS are considered (multi-hop), but this is not considered since it is out of the scope of this study.

Finally, note that due to Eq. 2.1, the directivity of RIS elements has to be specified to obtain more meaningful results. Based on [27], we have:

$$D_{element}(\theta) = \begin{cases} \frac{2}{\pi^2} sin^2(\theta) & 0 \leq \theta \leq \pi \\ 0 & \pi < \theta < 2\pi \end{cases} \tag{3.8}$$

Note that now Eq. 3.8 is a function of one variable, since, as stated in Sec. 3.1, a 2D case is studied.

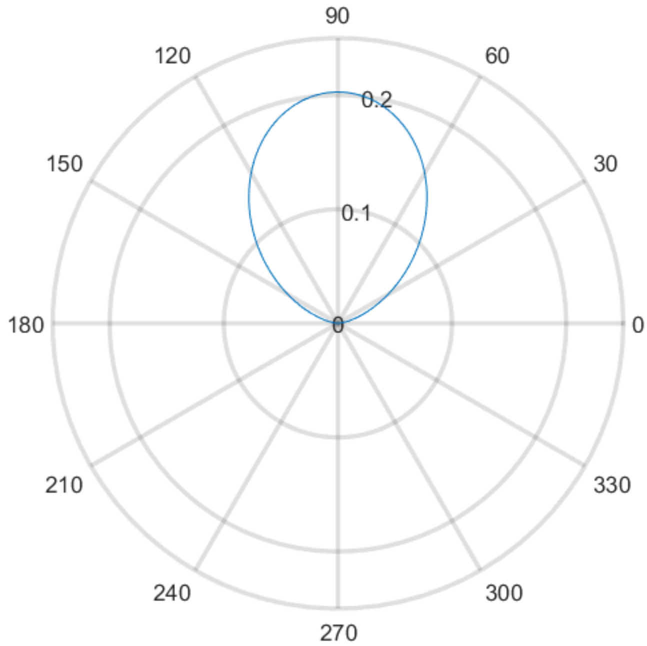

Figure 3.4: Polar plot of Eq. 3.8.

3.2.3 Small cell channel model

Two path losses are implemented (38.901 UMi LOS and NLOS). In this case, in order to avoid interference with BS, mmWaves are considered, and the central frequency is 30 GHz and it transmits with an EIRP of 40 W. The power noise is computed in the same way as BS, but the bandwidth is supposed to be 200 MHz since mmWaves provide larger bandwidths than the sub6 band. The path loss equations are

$$P_{\text{LOS}}(dB) = -32.4 - 20 \cdot \log_{10}(f_c/10^9) - 21 \cdot \log_{10}(d) \tag{3.9}$$

$$P_{\text{NLOS}}(dB) = -32.4 - 20 \cdot \log_{10}(f_c/10^9) - 31.9 \cdot \log_{10}(d). \tag{3.10}$$

It is supposed that the small cell only serves the UE which can obtain a better SNR from it than the BS.

3.3 Optimal placement

The objective is to maximize the area whose SNR is larger than a specific threshold SNR_t. In a real deployment, the value of SNR_t is really dependent on the kind of provided service. In this thesis, it is decided to consider SNR_t = 15dB [28].

In the case of deploying only one RIS, the optimal deployment will be done through a grid-search algorithm. The RIS will be placed in each position of the grid. For each position, multiple orientations of the RIS are considered. Specifically, the distance between two points of the grid is 20 meters, starting from point (0,0) to (280, 280), providing us with 15x15 = 225 points to test the RIS. The considered orientations are [0º,10º,20º,...,350º], where the orientation is the tilt of RIS surface with respect to the x-axis. For each point and orientation, the channel model is applied, obtaining a value of coverage. With it, the most optimal placement is found.

In the case of deploying multiple RIS, we implement a sub-optimal solution. First, only one RIS is considered and only its optimal positioning is considered. Once it is found, the RIS is placed there and the optimal positioning of the next RIS is considered, and so on. The optimal solution is not considered since it would take a prohibitively long time: with the suboptimal solution, $225 \cdot \#RIS$ combinations of points are tested, whereas with the optimal $225^{\#RIS}$ combinations are tested, i.e. it scales exponentially with the number of RIS.

In the case of the small cell, in order to have a fair comparison with RIS deployments, optimal positioning is considered too, following the same grid-search algorithm. However, multiple small cell deployment is not studied in this thesis.

Chapter 4

Results

Three scenarios are considered to carry out the simulations, see Fig. 4.1. In these, supposing only a BS in position (300,300) m as explained in Ch. 3, the following coverages are obtained: Map 1 is 54% covered, Map 2 is 58% covered and Map 3 is 26% covered. The SNR maps are shown in Fig. 4.2.

When deploying a single RIS, it is supposed that the number of elements is 1024. When deploying multiple RIS, the 1024 elements are equally distributed between all the RIS: with 2, each has 512 elements and with 3, each has 341.

4.1 Centralized RIS deployment

In Fig. 4.3, maps of the optimal positioning of a RIS are shown. The brighter the position, the larger the coverage provided by the RIS. It can be noticed that in all maps, the best positions are the points closer to the out-of-coverage zones shown in Fig. 4.2 when only the BS is deployed. On the other hand, it can be seen, especially in Map 3, how the RIS optimal positions tend to be in the vicinity of the boundary between covered and out-of-coverage points in Fig. 4.2. In Fig. 4.4, the best orientation for RIS in each position is provided. In Fig. 4.5, the resulting SNR maps are shown, obtaining the following maximum values of coverage when the RIS is optimally deployed: 71% for Map 1, 73% for Map 2 and 44% for Map 3. This is an improvement of 17%, 14% and 18% respectively.

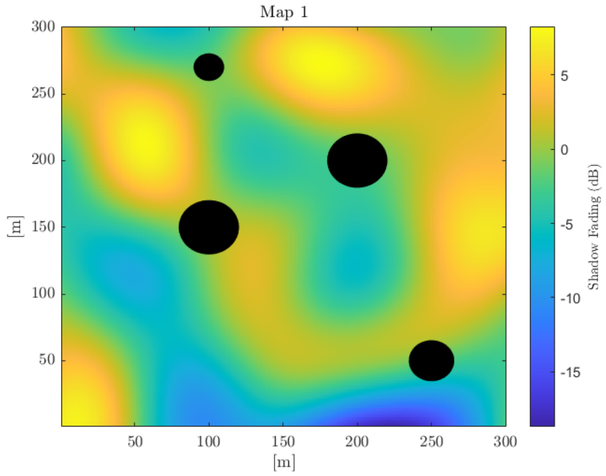

(a) Scenario 1.

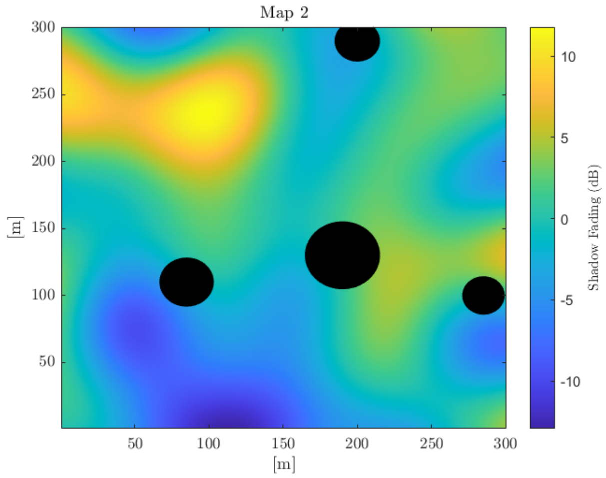

(b) Scenario 2.

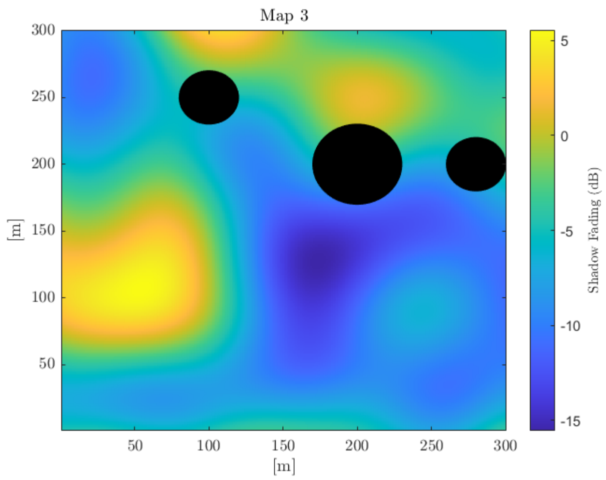

(c) Scenario 3.

Figure 4.1: Considered scenarios: shadow fading and obstacles.

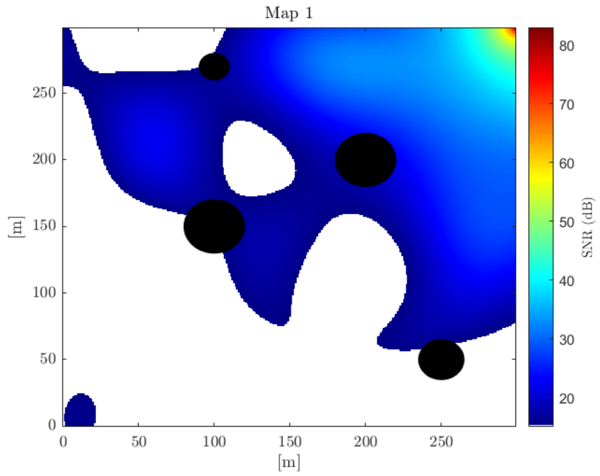

(a) Map 1. Coverage = 54%.

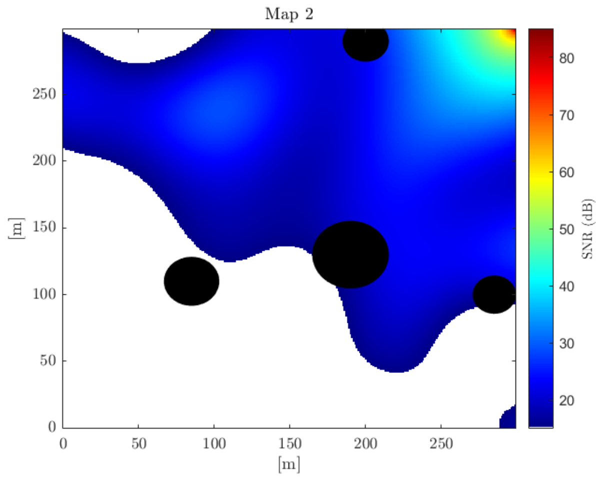

(b) Map 2. Coverage = 58%.

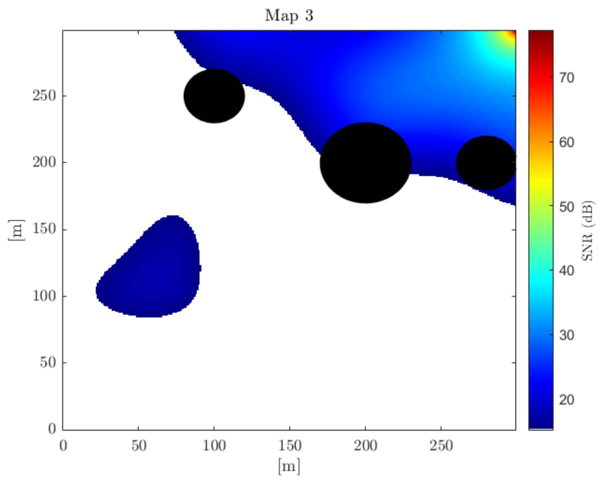

(c) Map 3. Coverage = 26%.

Figure 4.2: SNR maps with only BS. In white, the points whose $SNR < SNR_t$, i.e. out of coverage zones.

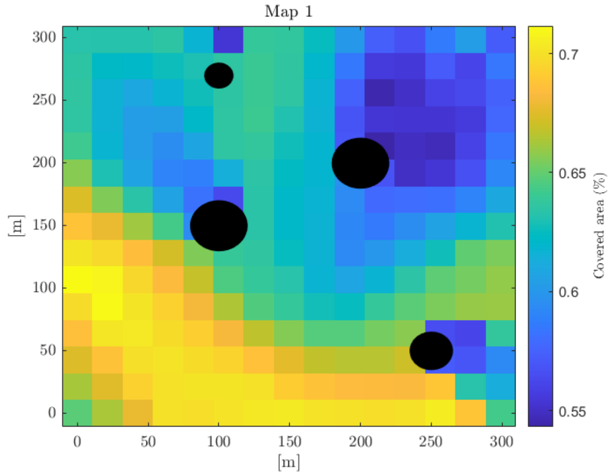

(a) Map 1.

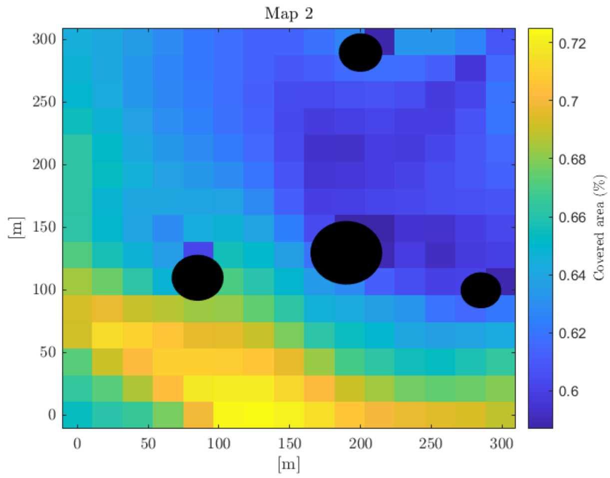

(b) Map 2.

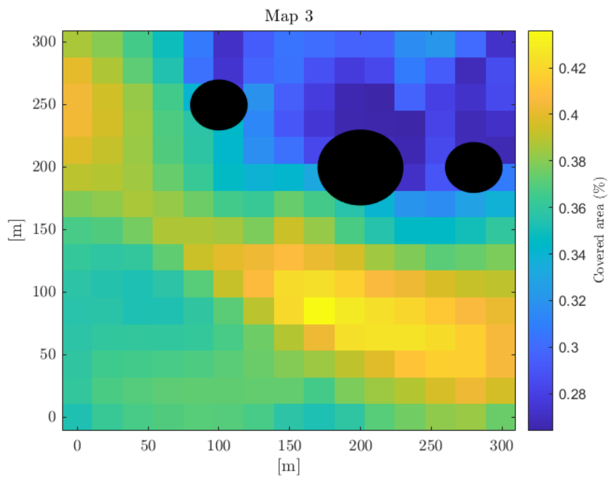

(c) Map 3.

Figure 4.3: Maps of optimal positioning of RIS. The brighter the position, the larger the coverage when RIS is placed in that position.

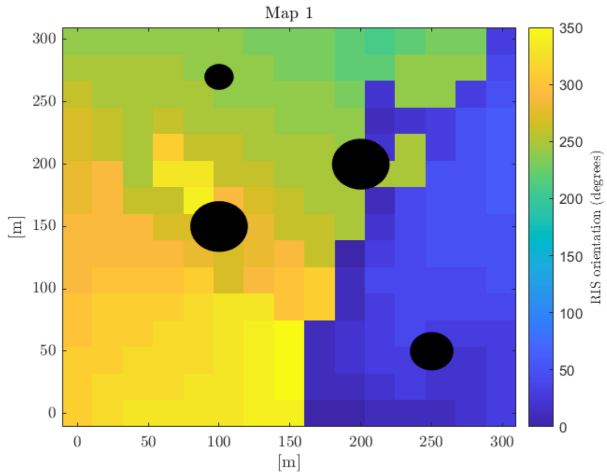

(a) Map 1.

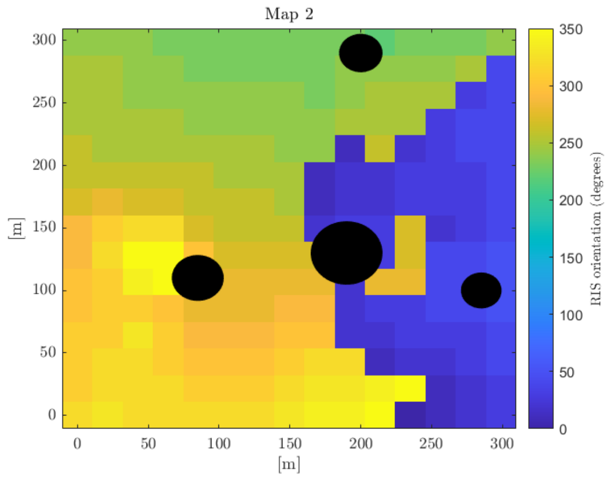

(b) Map 2.

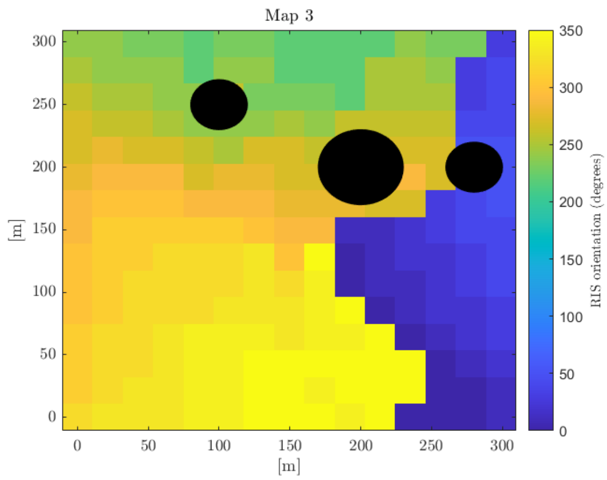

(c) Map 3.

Figure 4.4: Maps of optimal orientation of RIS (slope of RIS plane with respect to x-axis) in each position.

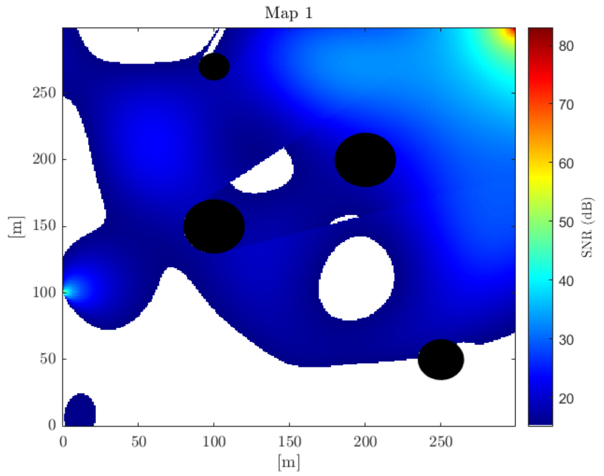

(a) Map 1. Coverage = 71%.

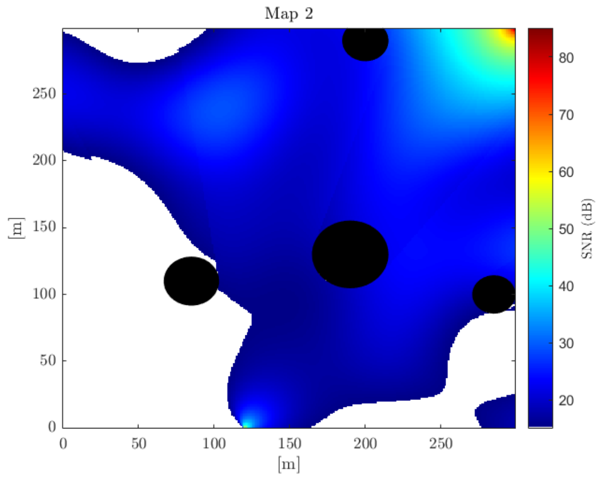

(b) Map 2. Coverage = 73%.

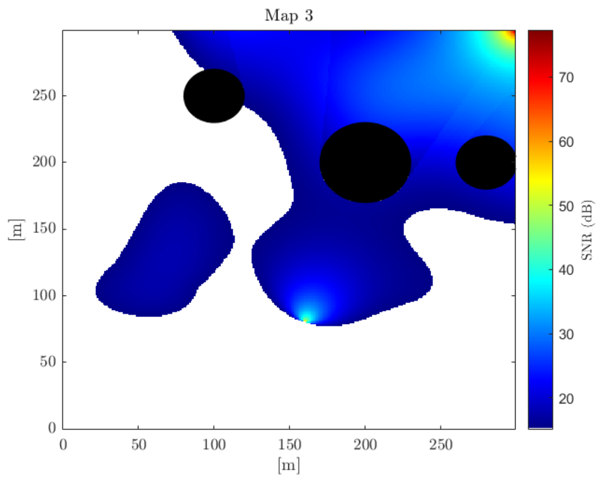

(c) Map 3. Coverage = 44%.

Figure 4.5: SNR map with RIS optimally placed and orientated.

4.2 Distributed RIS deployment

4.2.1 2 RIS

In Fig. 4.6, 4.7 and 4.8, it is shown the positioning procedure of two RIS for Map 1, 2 and 3 respectively. Once RIS number one is optimally placed, RIS number two is placed with RIS one deployed in the most optimal position, as explained in Ch. 3. In Fig. 4.9, the resulting SNR maps are shown, obtaining the following maximum values of coverage: 70% for Map 1, 73% for Map 2 and 41% for Map 3. This is an improvement of 16%, 14% and 15% respectively. Note that generally, the improvement is the same or worse than centralized deployment.

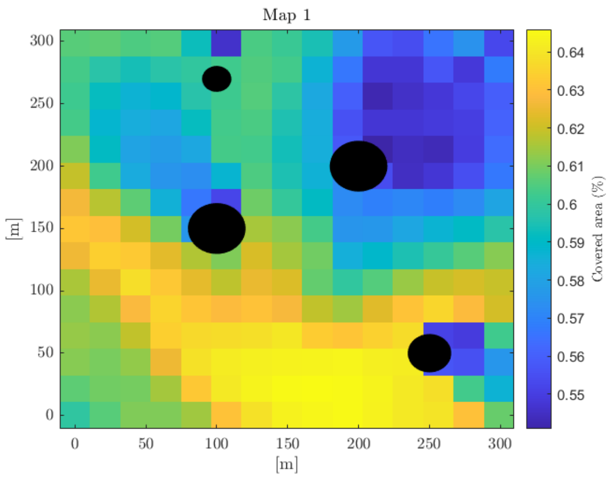

(a) Optimal positioning of RIS number 1.

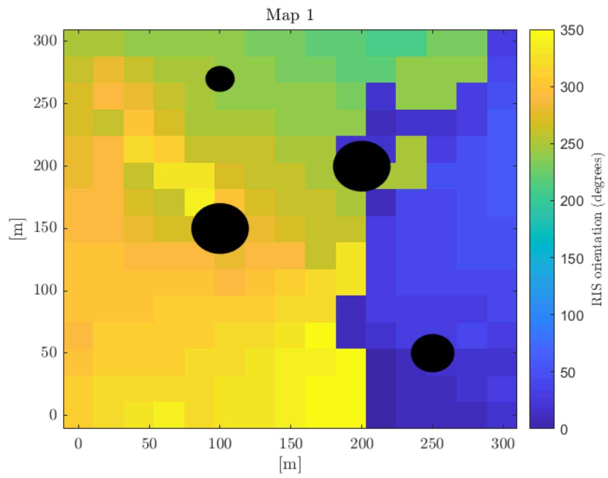

(b) Optimal orientation of RIS number 1.

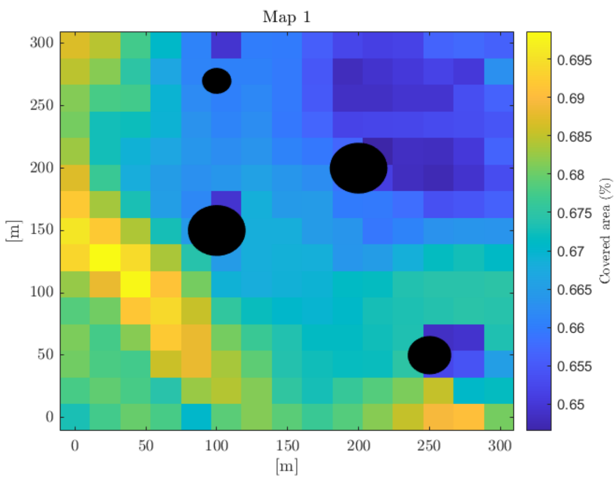

(c) Optimal positioning of RIS number 2.

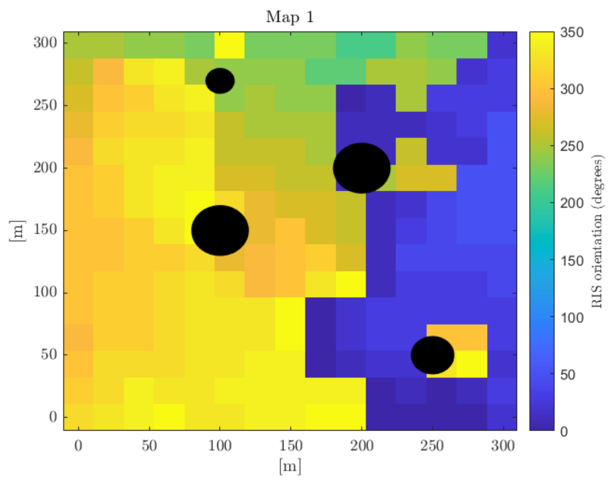

(d) Optimal orientation of RIS number 2.

Figure 4.6: Results of optimization of 2 RIS placement in scenario 1.

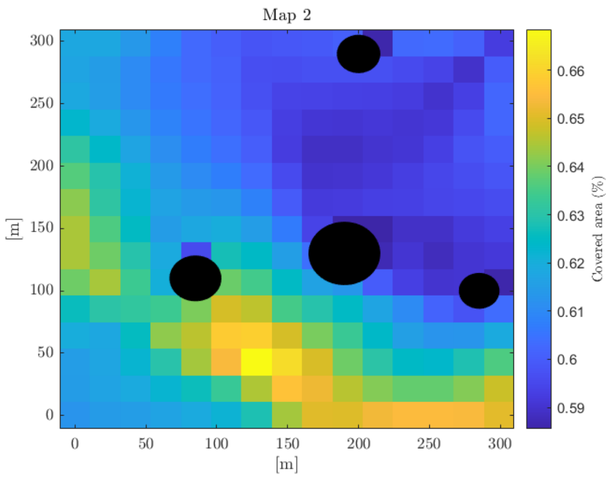

(a) Optimal positioning of RIS number 1.

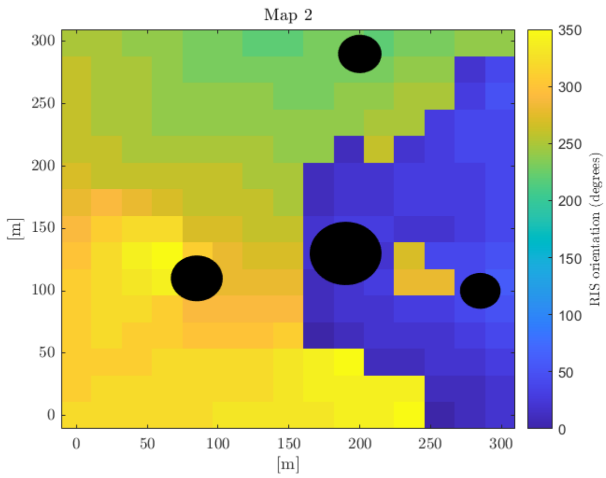

(b) Optimal orientation of RIS number 1.

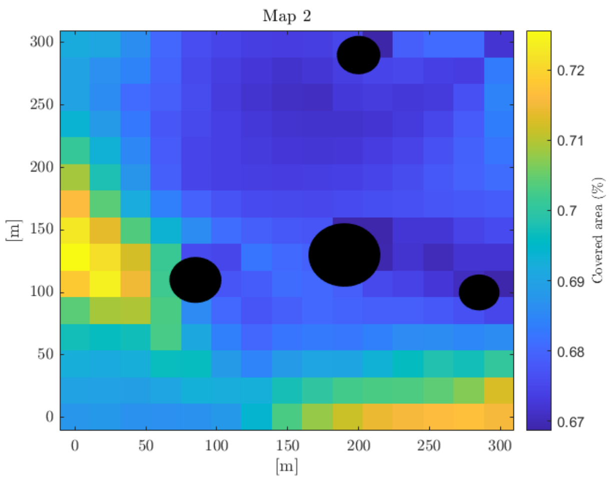

(c) Optimal positioning of RIS number 2.

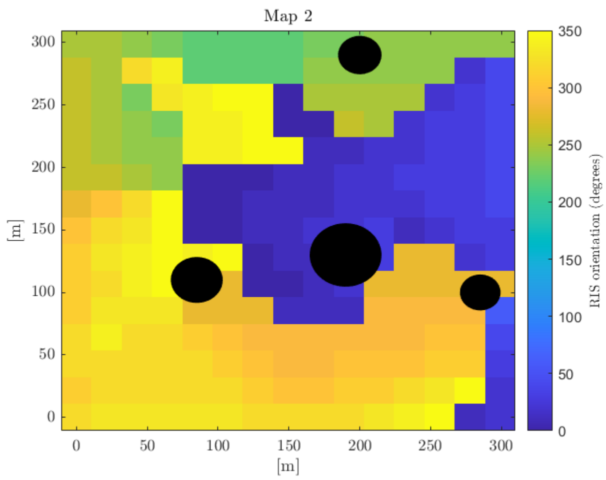

(d) Optimal orientation of RIS number 2.

Figure 4.7: Results of optimization of 2 RIS placement in scenario 2.

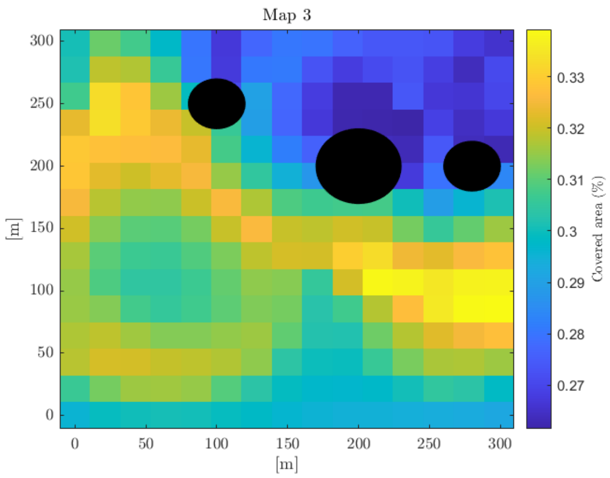

(a) Optimal positioning of RIS number 1.

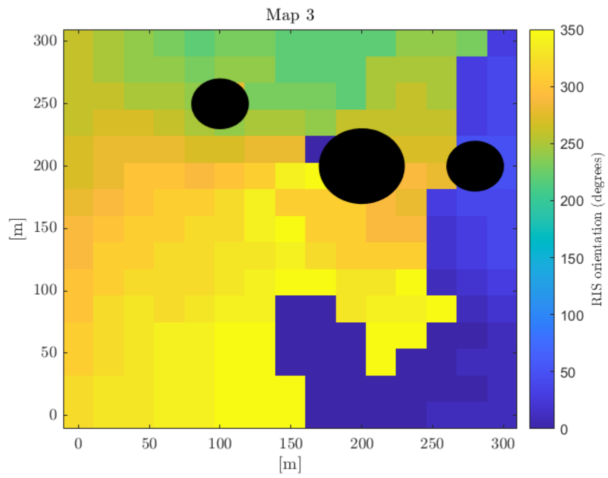

(b) Optimal orientation of RIS number 1.

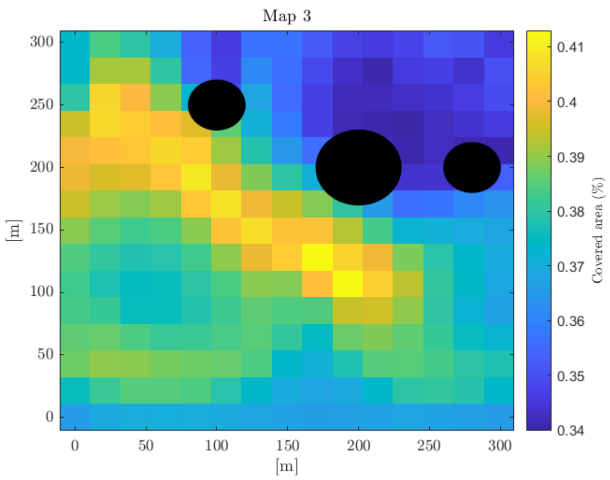

(c) Optimal positioning of RIS number 2.

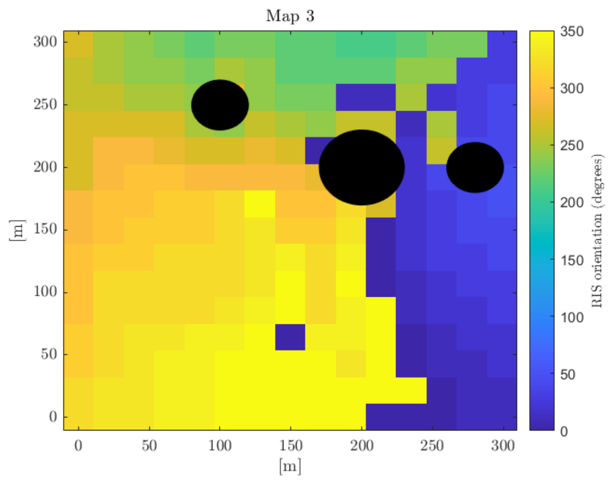

(d) Optimal orientation of RIS number 2.

Figure 4.8: Results of optimization of 2 RIS placement in scenario 3.

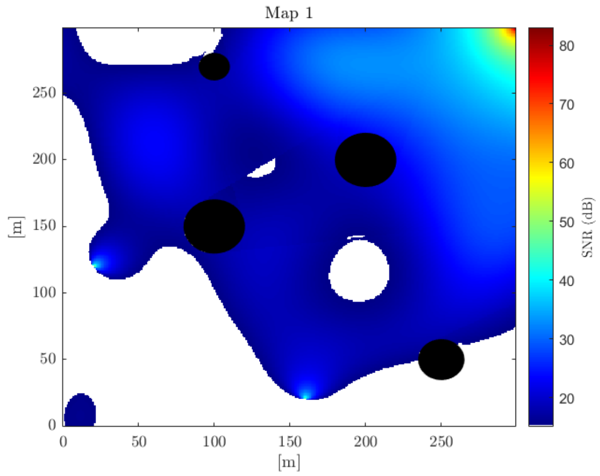

(a) Map 1. Coverage = 70%.

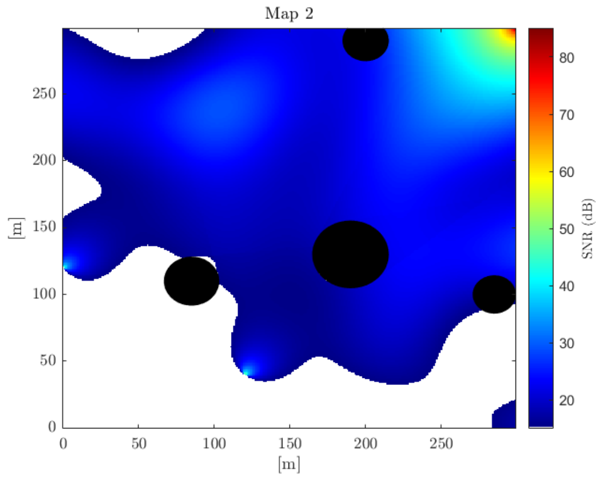

(b) Map 2. Coverage = 73%.

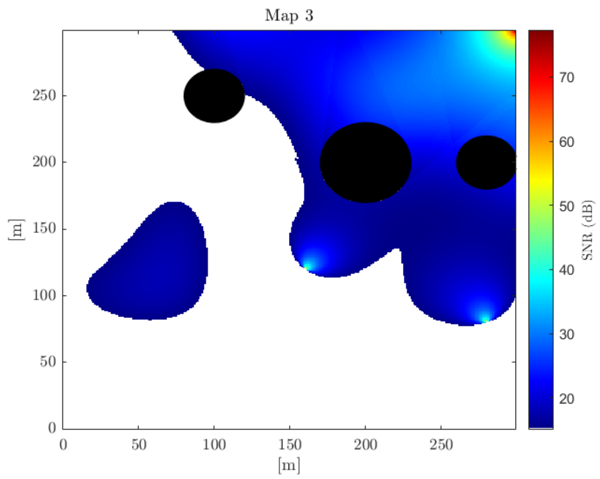

(c) Map 3. Coverage = 41%.

Figure 4.9: SNR map with 2 RIS optimally placed and orientated.

4.2.2 3 RIS

In Fig. 4.10, 4.11 and 4.12, it is shown the positioning procedure of three RIS for Map 1, 2 and 3 respectively. Once RIS number one is optimally placed, RIS number two is placed with RIS one deployed in the most optimal position, and so RIS number three. In 4.9, the resulting SNR maps are shown, obtaining the following maximum values of coverage: 69% for Map 1, 72% for Map 2 and 41% for Map 3. This is an improvement of 15%, 14% and 15% respectively. Note that generally, the improvement is worse than the 2-RIS and centralized.

4.3 Small cell comparison

In Fig. 4.14, the optimal positioning of the small cell is shown for each map. The coverage for Map 1 is 84%, for Map 2 is 85% and for Map 3 is 65%. The comparison of RIS was performed with centralized RIS since it is the most optimal configuration. In all three maps, it is concluded that RIS would need 2700 elements to match small cell coverage. Taking into account that RIS operates with a central frequency of 3.5 GHz, supposing a typical spacing between elements in a square RIS of $\lambda/2$ [29] and considering the size of each element as $\lambda/5$ [30], we obtain a RIS of side length equal to 2.6 meters, this is a surface of 6.76 m^2. In Fig. 4.15, a comparison between SNR maps by small cells and RIS is shown. It has to be noted that the optimal placement varies with the number of RIS elements. In the previous results, it varies slightly, but as we increase it significantly, the optimal position tends to move further from the vicinity of the boundary between covered and uncovered zones.

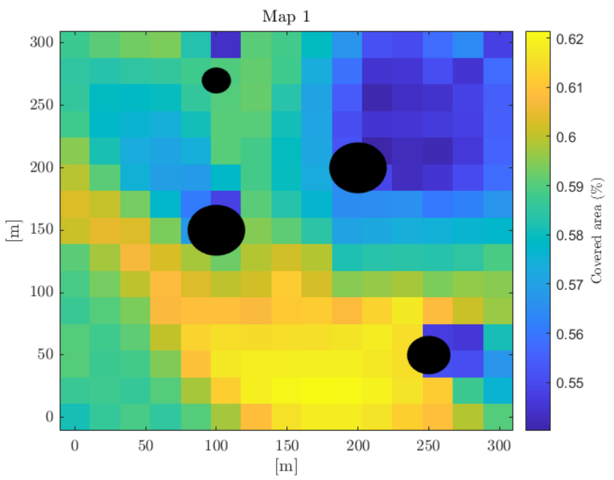

(a) Optimal positioning of RIS number 1.

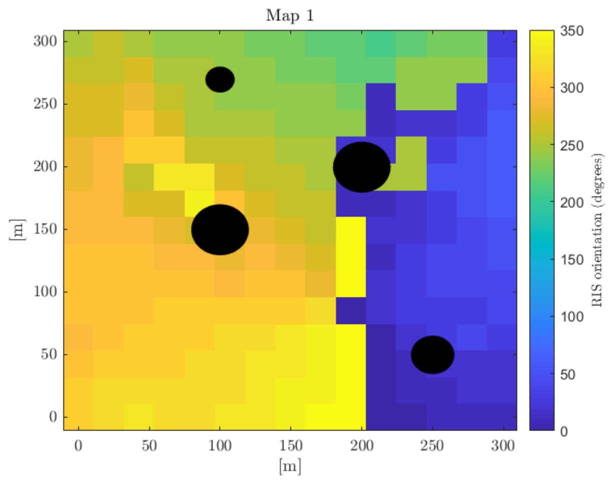

(b) Optimal orientation of RIS number 1.

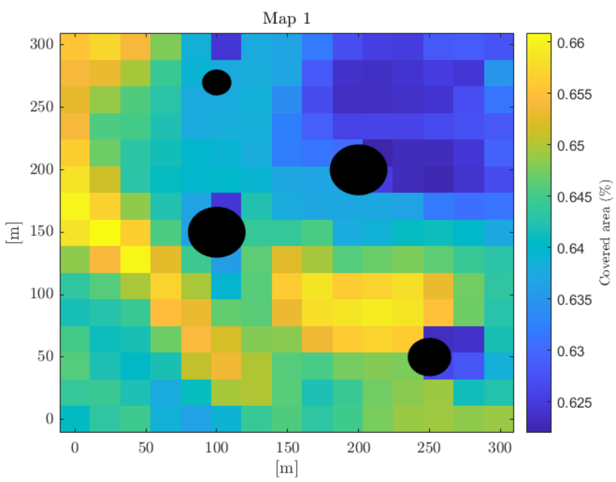

(c) Optimal positioning of RIS number 2.

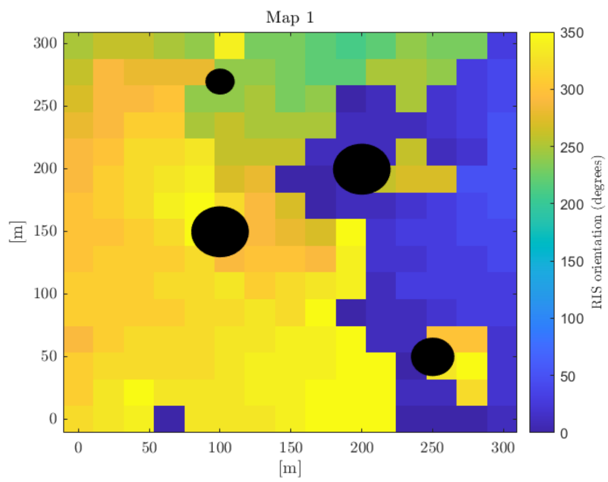

(d) Optimal orientation of RIS number 2.

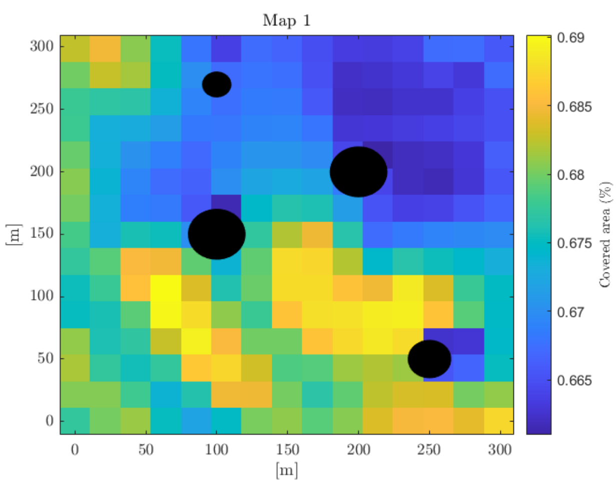

(e) Optimal positioning of RIS number 3.

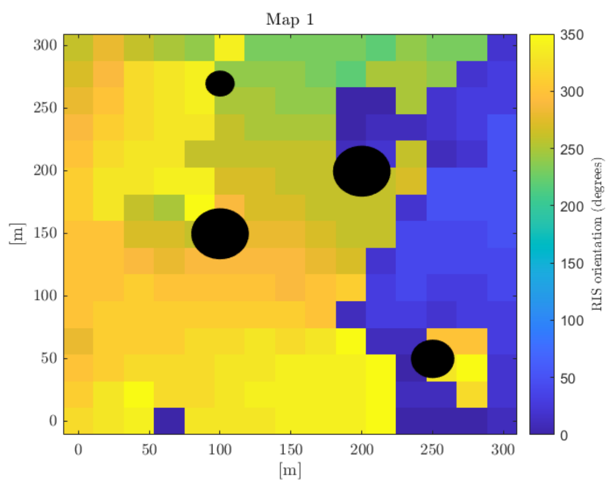

(f) Optimal orientation of RIS number 3.

Figure 4.10: Results of optimization of 3 RIS placement in scenario 1.

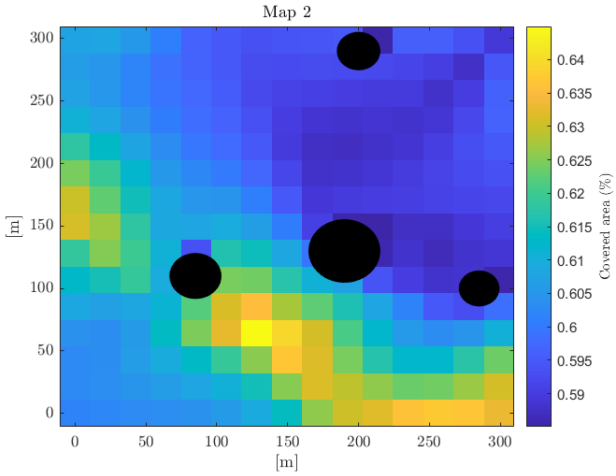

(a) Optimal positioning of RIS number 1.

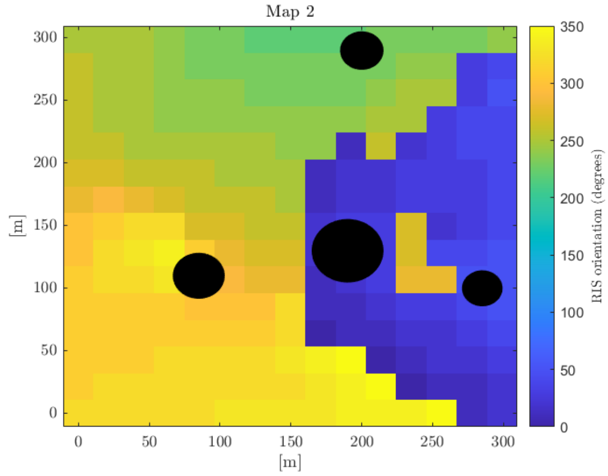

(b) Optimal orientation of RIS number 1.

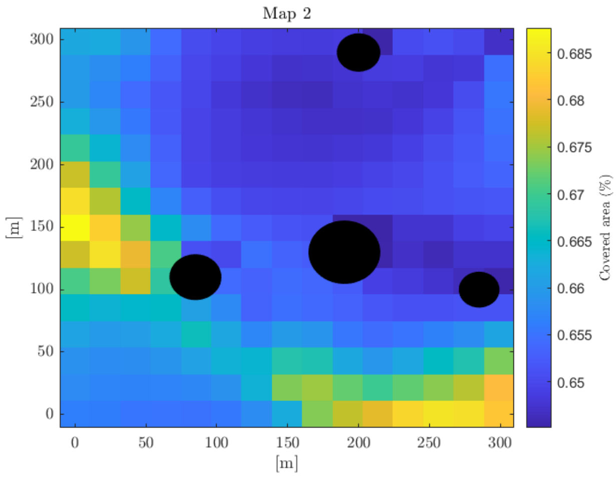

(c) Optimal positioning of RIS number 2.

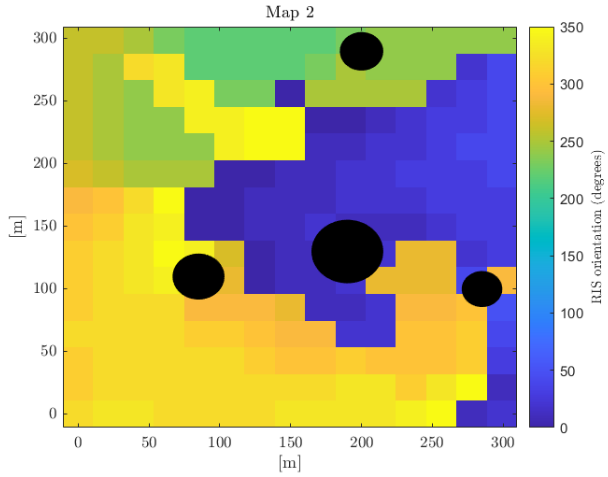

(d) Optimal orientation of RIS number 2.

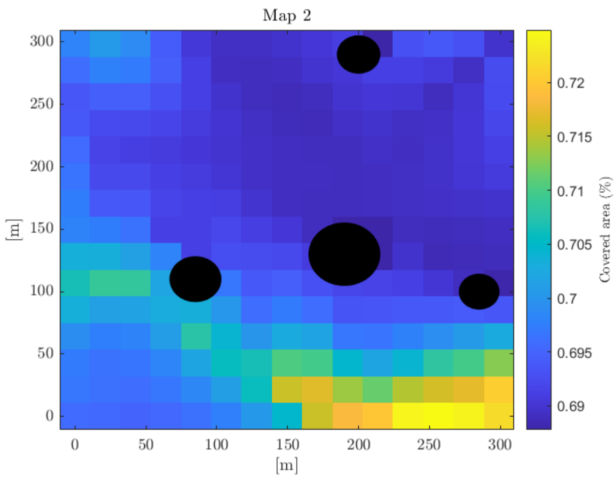

(e) Optimal positioning of RIS number 3.

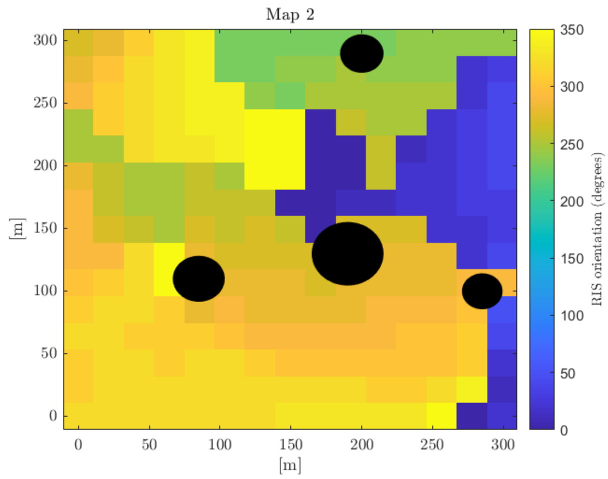

(f) Optimal orientation of RIS number 3.

Figure 4.11: Results of optimization of 3 RIS placement in scenario 2.

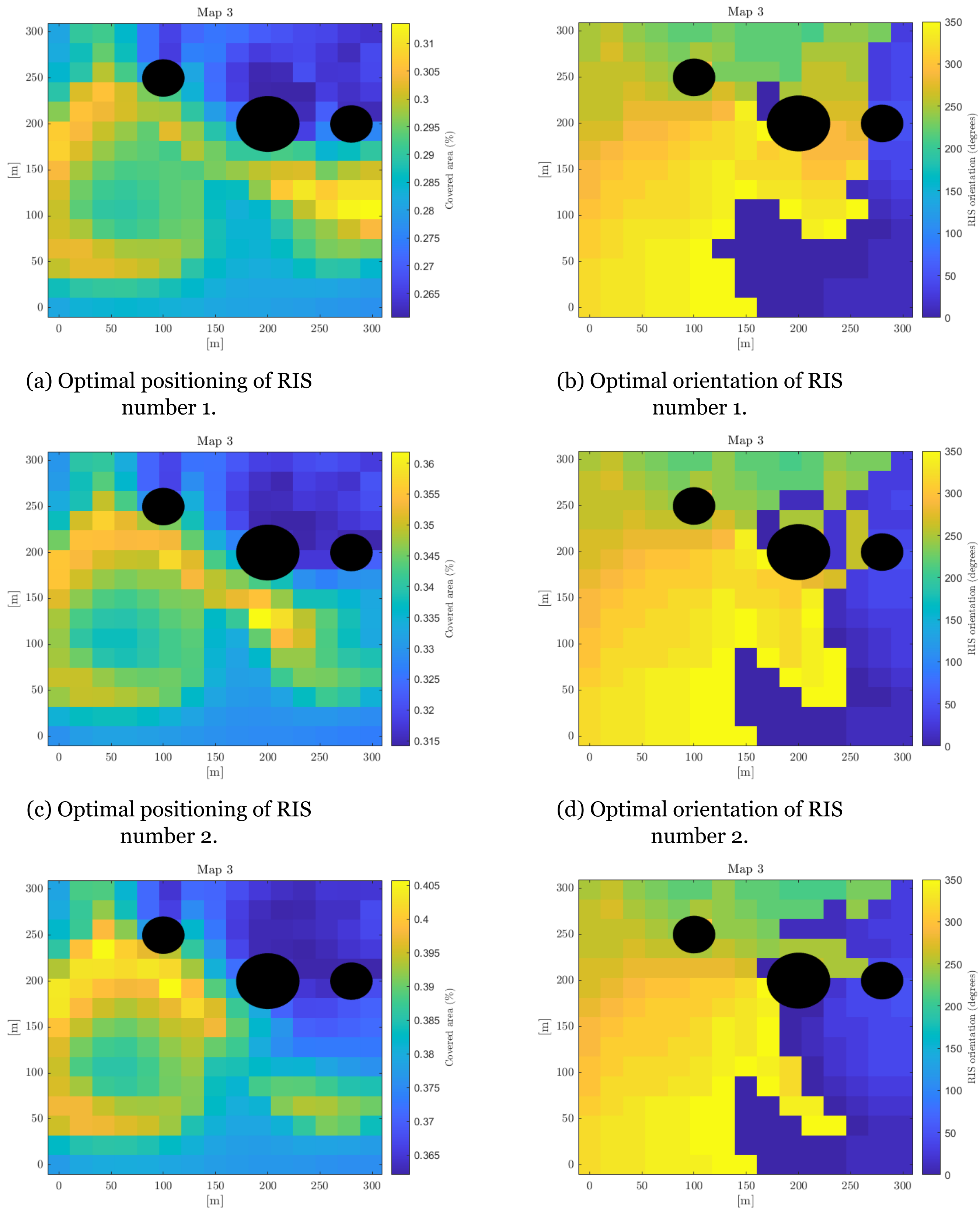

(a) Optimal positioning of RIS number 1.

(b) Optimal orientation of RIS number 1.

(c) Optimal positioning of RIS number 2.

(d) Optimal orientation of RIS number 2.

(e) Optimal positioning of RIS number 3.

(f) Optimal orientation of RIS number 3.

Figure 4.12: Results of optimization of 3 RIS placement in scenario 3.

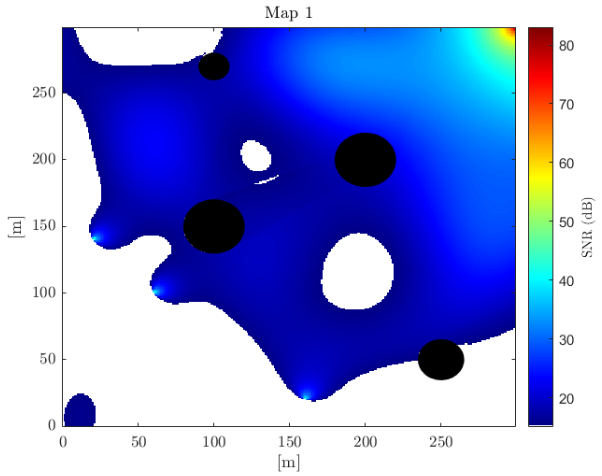

(a) Map 1. Coverage = 69%.

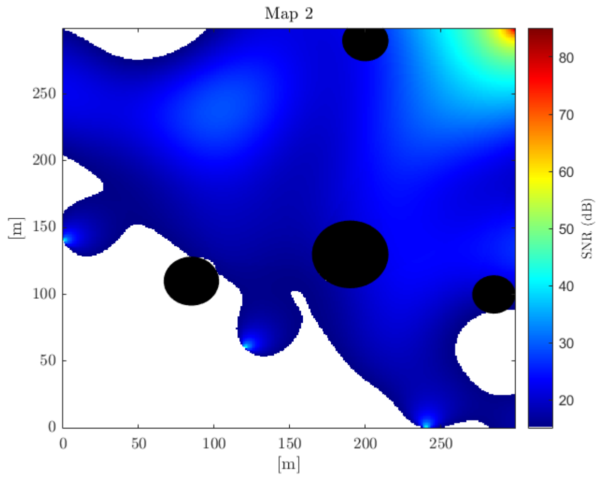

(b) Map 2. Coverage = 72%.

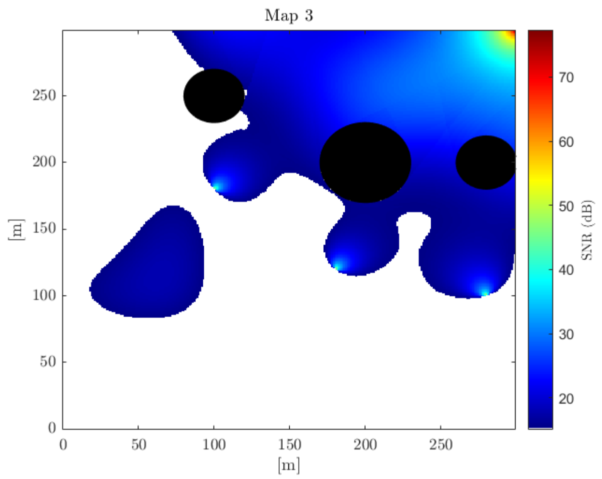

(c) Map 3. Coverage = 41%.

Figure 4.13: SNR map with 3 RIS optimally placed and orientated.

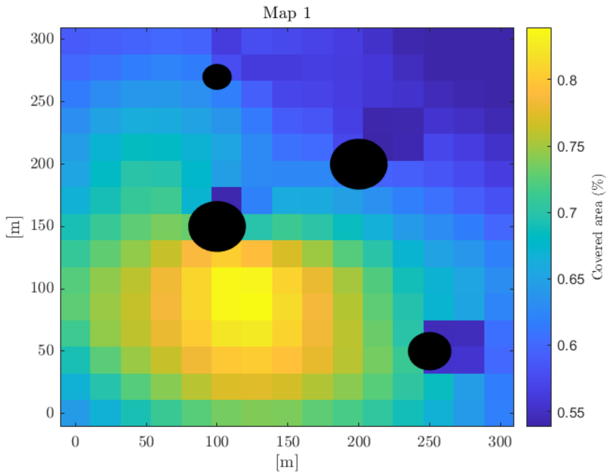

(a) Map 1.

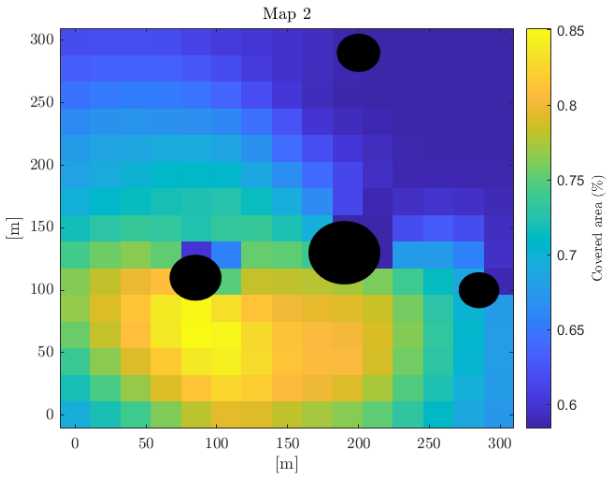

(b) Map 2.

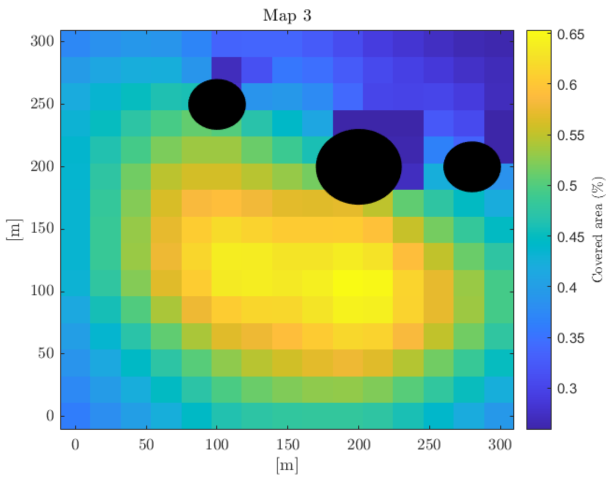

(c) Map 3.

Figure 4.14: Optimal positioning and coverage values for a small cell.

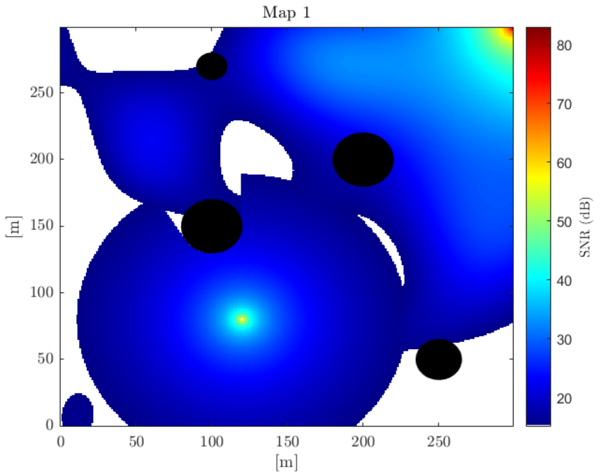

(a) Map 1.

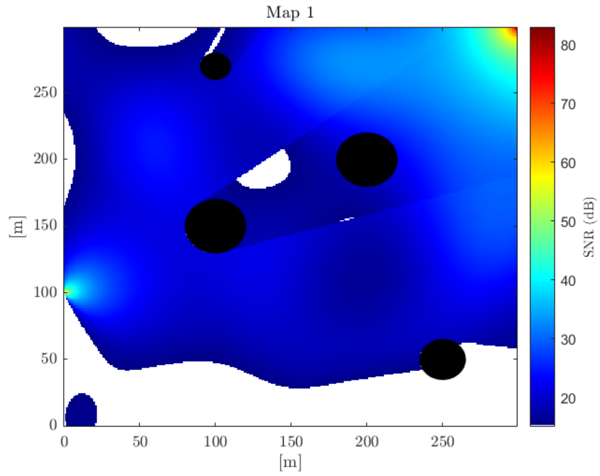

(b) Map 1.

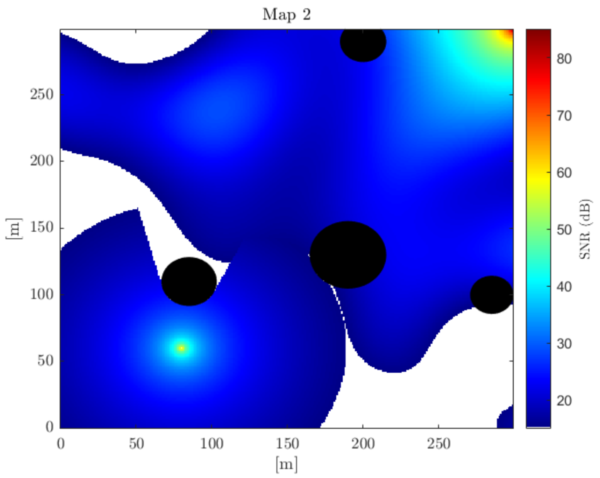

(c) Map 2.

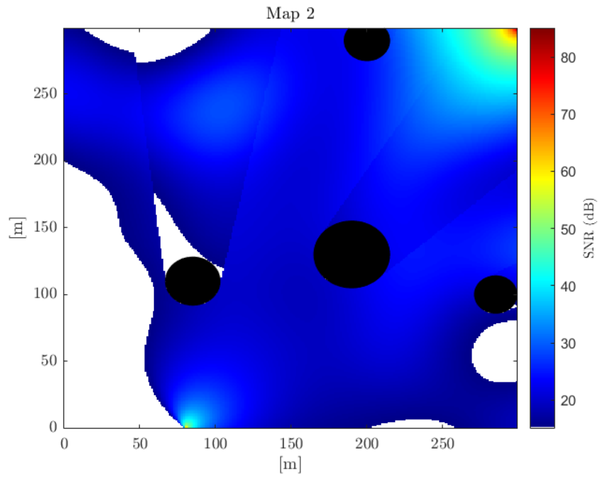

(d) Map 2.

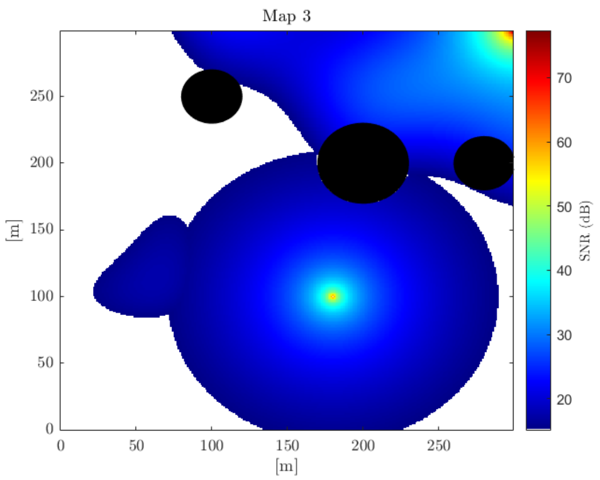

(e) Map 3.

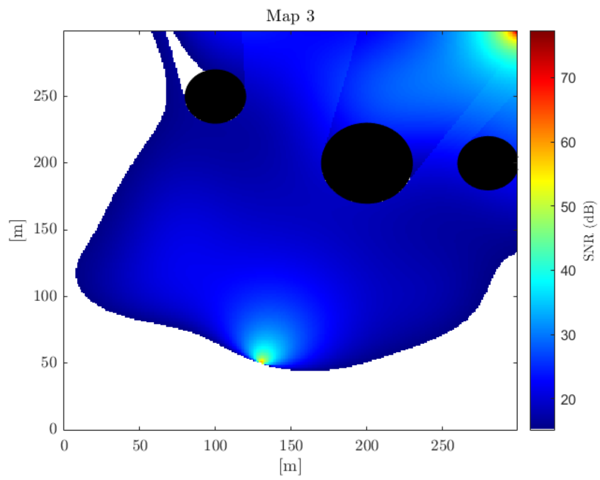

(f) Map 3.

Figure 4.15: SNR maps: at right a small cell is depolyed and at left a RIS with 2700 elements.

Chapter 5

Conclusions

In this thesis, we study the optimal strategies for the deployment of RIS in terms of coverage in an outdoor urban scenario. To do so, we answer three questions: 1. Which is the best positioning and orientation of RIS in a propagation environment? 2. Is it better to deploy only a RIS with M elements or several with a total number of M elements? 3. How many elements does RIS need to match the coverage capabilities of a small cell?

With the performed simulations, we obtain the following conclusions. Firstly, the optimal positioning of RIS lies in the out-of-coverage zone, and more specifically in the vicinity of the boundary between covered and out-of-coverage zones. Secondly, it can be seen that centralized deployment is better than distributed schemes, even though the difference in coverage improvement is quite small. Finally, regarding the small cell comparison, we find that in the provided maps a RIS of 2700 elements suffices to match the small cell coverages, which suggests that a RIS with a feasible number of elements could replace small cells in terms of SNR coverage since the resulting RIS surface size is 6.76 m^2.

Future research directions on the topic could be the study of the optimal placement considering multi-hop RIS and the consideration of other meaningful metrics beyond SNR such as throughput.

Bibliography

[1] Björnson, Emil, Wymeersch, Henk, Matthiesen, Bho, Popovski, Petar, Sanguinetti, Luca, and Carvalho, Elisabeth de. "Reconfigurable Intelligent Surfaces: A signal processing perspective with wireless applications". In: *IEEE Signal Processing Magazine* 39.2 (2022), pp. 135–158. DOI: 10.1109/MSP.2021.3130549.

[2] Björnson, Emil, Özdogan, Özgecan, and Larsson, Erik G. "Reconfigurable Intelligent Surfaces: Three Myths and Two Critical Questions". In: *CoRR* abs/2006.03377 (2020). arXiv: 2006.03377. URL: https://arxiv.org/abs/2006.03377.

[3] Enqvist, Anders, Tuğfe Demir, Özlem, Cavdar, Cicek, and Björnson, Emil. "Optimizing Reconfigurable Intelligent Surfaces for Small Data Packets: A Subarray Approach". In: *ICC 2022 - IEEE International Conference on Communications*. 2022, pp. 2664–2669. DOI: 10.1109/ICC45855.2022.9839247.

[4] Huang, Chongwen, Zappone, Alessio, Alexandropoulos, George C., Debbah, Mérouane, and Yuen, Chau. "Reconfigurable Intelligent Surfaces for Energy Efficiency in Wireless Communication". In: *IEEE Transactions on Wireless Communications* 18.8 (2019), pp. 4157–4170. DOI: 10.1109/TWC.2019.2922609.

[5] Shi, Shuai, Wang, Lei, and Jonsson, Lars. "Antenna Current Optimization using Semidefinite Relaxation". In: (Nov. 2017).

[6] Scepanskis, Mihails. *Simulating a parabolic antenna for satellite communications*. Nov. 2021. URL: https://www.cenos-platform.com/post/simulating-a-parabolic-antenna-for-satellite-communications.

[7] Lotter, M.P. and Van Rooyen, P. “An overview of space division multiple access techniques in cellular systems”. In: *Proceedings of the 1998 South African Symposium on Communications and Signal Processing-COMSIG ’98 (Cat. No. 98EX214)*. 1998, pp. 161–164. DOI: 10.1109/COMSIG.1998.736941.

[8] Marzetta, Thomas L. *Fundamentals of massive mimo*. Cambridge University Press, 2016.

[9] Björnson, Emil. URL: https://github.com/emilbjornson.

[10] Romeu Robert, J., Cardama Aznar, Á., and Blanch Boris, S. *Antenas*. Universitat Politecnica de Catalunya. Iniciativa Digital Politecnica, 2004. ISBN: 9788483019900. URL: https://books.google.se/books?id=MBGiCgAAQBAJ.

[11] Dai, Linglong, Wang, Bichai, Wang, Min, Yang, Xue, Tan, Jingbo, Bi, Shuangkaisheng, Xu, Shenheng, Yang, Fan, Chen, Zhi, Renzo, Marco Di, Chae, Chan-Byoung, and Hanzo, Lajos. “Reconfigurable Intelligent Surface-Based Wireless Communications: Antenna Design, Prototyping, and Experimental Results”. In: *IEEE Access* 8 (2020), pp. 45913–45923. DOI: 10.1109/ACCESS.2020.2977772.

[12] Pei, Xilong, Yin, Haifan, Tan, Li, Cao, Lin, Li, Zhanpeng, Wang, Kai, Zhang, Kun, and Björnson, Emil. *RIS-Aided Wireless Communications: Prototyping, Adaptive Beamforming, and Indoor/Outdoor Field Trials*. 2021. arXiv: 2103.00534 [cs.IT].

[13] Kishk, Mustafa A. and Alouini, Mohamed-Slim. *Exploiting Randomly-located Blockages for Large-Scale Deployment of Intelligent Surfaces*. 2020. arXiv: 2001.10766 [cs.IT].

[14] Liu, Yuanwei, Liu, Xiao, Mu, Xidong, Hou, Tianwei, Xu, Jiaqi, Di Renzo, Marco, and Al-Dhahir, Naofal. “Reconfigurable Intelligent Surfaces: Principles and Opportunities”. In: (2020). DOI: 10.48550/ARXIV.2007.03435. URL: https://arxiv.org/abs/2007.03435.

[15] Pan, Cunhua, Ren, Hong, Wang, Kezhi, Kolb, Jonas Florentin, Elkashlan, Maged, Chen, Ming, Di Renzo, Marco, Hao, Yang, Wang, Jiangzhou, Swindlehurst, A. Lee, You, Xiaohu, and Hanzo, Lajos. “Reconfigurable Intelligent Surfaces for 6G Systems: Principles, Applications, and Research Directions”. In: *IEEE Communications Magazine* 59.6 (2021), pp. 14–20. DOI: 10.1109/MCOM.001.2001076.

[16] Wu, Qingqing, Zhang, Shuowen, Zheng, Beixiong, You, Changsheng, and Zhang, Rui. "Intelligent Reflecting Surface Aided Wireless Communications: A Tutorial". In: (2020). DOI: 10.48550/ARXIV.2007.02759. URL: https://arxiv.org/abs/2007.02759.

[17] Wu, Qingqing and Zhang, Rui. "Towards Smart and Reconfigurable Environment: Intelligent Reflecting Surface Aided Wireless Network". In: *IEEE Communications Magazine* 58.1 (2020), pp. 106–112. DOI: 10.1109/MCOM.001.1900107.

[18] Al-Nahhas, Bayan, Obeed, Mohannad, Chaaban, Anas, and Hossain, Md. Jahangir. "Ris-aided cell-free massive MIMO: Performance analysis and competitiveness". In: *2021 IEEE International Conference on Communications Workshops (ICC Workshops)* (2021). DOI: 10.1109/iccworkshops50388.2021.9473521.

[19] Stratidakis, Giorgos, Droulias, Sotiris, and Alexiou, Angeliki. "Optimal Position and Orientation Study of Reconfigurable Intelligent Surfaces in a Mobile User Environment". In: *IEEE Transactions on Antennas and Propagation* 70.10 (2022), pp. 8863–8871. DOI: 10.1109/TAP.2022.3208036.

[20] Ntontin, Konstantinos, Boulogeorgos, Alexandros-Apostolos A., Selimis, Dimitrios, Lazarakis, Fotis, Alexiou, Angeliki, and Chatzinotas, Symeon. *Reconfigurable Intelligent Surface Optimal Placement in Millimeter-Wave Networks*. 2021. arXiv: 2011.09949 [cs.IT].

[21] Zhang, Shuowen and Zhang, Rui. *Intelligent Reflecting Surface Aided Multi-User Communication: Capacity Region and Deployment Strategy*. 2021. arXiv: 2009.02324 [cs.IT].

[22] Hossain, Ferdous, Geok, Tan Kim, Rahman, Tharek Abd, Hindia, Mohammad Nour, Dimyati, Kaharudin, Ahmed, Sharif, Tso, Chih P., and Abd Rahman, Noor Ziela. "An Efficient 3-D Ray Tracing Method: Prediction of Indoor Radio Propagation at 28 GHz in 5G Network". In: *Electronics* 8.3 (2019). ISSN: 2079-9292. DOI: 10.3390/electronics8030286. URL: https://www.mdpi.com/2079-9292/8/3/286.

[23] Bjornson, Emil and Sanguinetti, Luca. “Rayleigh Fading Modeling and Channel Hardening for Reconfigurable Intelligent Surfaces”. In: *IEEE Wireless Communications Letters* 10.4 (Apr. 2021), pp. 830–834. DOI: 10.1109/lwc.2020.3046107. URL: https://doi.org/10.1109%2Flwc.2020.3046107.

[24] Torres, Andrea De Jesus, Sanguinetti, Luca, and Björnson, Emil. *Intelligent Reconfigurable Surfaces vs. Decode-and-Forward: What is the Impact of Electromagnetic Interference?* 2022. arXiv: 2203.08046 [cs.IT].

[25] URL: https://quadriga-channel-model.de/.

[26] Dorokhin, Semyon, Lysov, Pavel, Aderkina, Anastasia, and Lyashev, Vladimir. *Reconfigurable Intelligent Surface MIMO Simulation using Quasi Deterministic Radio Channel Model*. 2022. arXiv: 2211.12601 [eess.SP].

[27] Droulias, Sotiris and Alexiou, Angeliki. *Reconfigurable Intelligent Surface: MIMO or radiating sheet?* 2023. arXiv: 2205.08819 [physics.app-ph].

[28] Apr. 2023. URL: https://documentation.meraki.com/MR/Wi-Fi_Basics_and_Best_Practices/Signal-to-Noise_Ratio_(SNR)_and_Wireless_Signal_Strength.

[29] Li, Zan, Kundu, Neel Kanth, Rao, Junhui, Shen, Shanpu, McKay, Matthew R., and Murch, Ross. “Performance Analysis of RIS-Assisted Communications With Element Grouping and Spatial Correlation”. In: *IEEE Wireless Communications Letters* 12.4 (2023), pp. 630–634. DOI: 10.1109/LWC.2023.3237232.

[30] Mohammadi Estakhri, Nasim and Alù, Andrea. “Wave-front Transformation with Gradient Metasurfaces”. In: *Phys. Rev. X* 6 (4 Oct. 2016), p. 041008. DOI: 10.1103/PhysRevX.6.041008. URL: https://link.aps.org/doi/10.1103/PhysRevX.6.041008.